Original Paper

phys. stat. sol. (b), **243**, No. 15, 3993–3997 (2006) / **DOI** 10.1002/pssb.200671610

Intraband photodetection at 1.3–1.5 μm in self-organized GaN/AlN quantum dots

L. Doyennette[*, 1], **A. Vardi**[2], **F. Guillot**[3], **L. Nevou**[1], **M. Tchernycheva**[1], **A. Lupu**[1], **R. Colombelli**[1], **G. Bahir**[2], **E. Monroy**[3], and **F. H. Julien**[1]

[1] Action OptoGaN, Institut d'Electronique Fondamentale, Université Paris-Sud, UMR 8622 CNRS, 91405 Orsay cedex, France
[2] Department of Electrical Engineering, Technion-Israel Institute of Technology, Haifa 32000, Israel
[3] Equipe mixte CEA-CNRS-UJF Nanophysique et Semiconducteurs, DRFMC/SP2M/PSC, CEA-Grenoble, 17 rue des Martyrs, 38054 Grenoble cedex 9, France

Received 1 May 2006, revised 14 June 2006, accepted 5 September 2006
Published online 25 October 2006

PACS 72.40.+w, 73.63.Kv, 78.66.Fd, 78.67.Hc, 81.16.Dn, 85.60.Gz

GaN/AlN quantum dot photodetectors based on intraband absorption and in-plane carrier transport have been fabricated and characterized. These photodetectors operate at room temperature at telecommunication wavelengths (1.3–1.55 μm). Their TM-polarized intraband absorption is ascribed to the transition from the ground state s to the excited state p_z of the GaN dots. The responsivity peaked at 1.41 μm is as high as 8 mA/W at room temperature for the interdigitated contact photodetector.

1 Introduction

III-nitride semiconductors are intensively studied for electronic and optoelectronic applications in the visible and ultraviolet spectral range because of their wide band gaps. Most of these optoelectronic devices rely on conduction to valence band (interband) transitions. However, III-nitride heterostructures such as quantum wells (QWs) or quantum dots (QDs) have a large conduction band offset (1.75 eV for GaN/AlN QWs), which is a key feature for tuning intersubband optical transitions in the near-infrared spectral range. Intersubband absorptions at 1.3–1.55 μm have already been reported at room temperature in ultra thin GaN/AlN QWs [1]. Intraband absorptions have been observed at room temperature in undoped and n-doped self-organized GaN/AlN QDs at fiber-optics communication wavelengths [2–4].

Quantum dots are of great interest for intraband photodetection [5, 6]. With respect to QW intersubband photodetectors, they should exhibit an intrinsically lower noise due to the reduction of electron–phonon scattering. Secondly, normal incidence photodetection is allowed because of the three-dimensional electronic confinement in the QDs. Regular quantum dots infrared photodetectors (QDIPs) are based on vertical transport of electrons. The photoexcited electrons tunnel into the continuum towards the contact under an applied bias. For in-plane QDIPs, the confined electrons are excited into the two-dimensional wetting layer (WL) and the photocurrent (PC) relies on lateral carrier transport. In-plane QDIPs have already been demonstrated in InAs/GaAs QDs [7].

In this paper, we report on GaN/AlN QDIPs based on intraband absorption and lateral carrier transport in the WL, operating at wavelengths as short as 1.37 μm at room temperature [8, 9]. The responsivity peaked at 1.41 μm is as high as 8 mA/W at room temperature for an interdigitated contact photodetector.

[*] Corresponding author: e-mail: laetitia.doyennette@ief.u-psud.fr, Phone: +33 1 69 15 40 51, Fax: +33 1 69 15 41 15

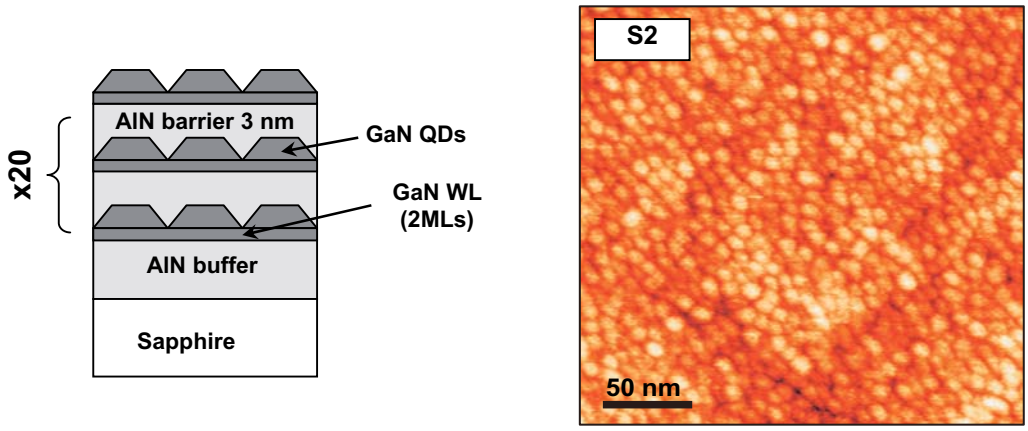

Fig. 1 (online colour at: www.pss-b.com) Left: scheme of S1, S2 and S3 structure. Right: atomic force microscopy image of the QDs deposited on the surface of the sample S2.

2 Sample growth

We have investigated three samples (S1, S2 and S3). They consist of 20 periods of Si-doped GaN QD layers separated by 3 nm-thick AlN barriers. They are grown on an AlN buffer of 1 μm on c-sapphire substrate by plasma-assisted molecular-beam epitaxy (PAMBE). The sample structure is described in Fig. 1. The growth of self-assembled QDs is achieved by the deposition of GaN on the AlN surface under N-rich conditions. Under these conditions, the growth starts in 2D mode (QWs) and switches to the 3D mode (QDs) after the deposition of a 2-monolayer-thick wetting layer (Stranski–Krastanov growth mode). Electron population of the QDs is provided by silicon doping of the GaN layer at a nominal concentration of 1×10^{20} cm^{-3}. The growth of the sample ends with a QD layer at the surface to allow atomic force microscopy characterizations (AFM). An AFM image of the QDs is presented in Fig. 1. The characteristics (density, height and diameter) of the QDs are summarized in Table 1. Further growth details will published elsewhere [4].

3 Device fabrication

The sample facets have been mechanically polished at a 45° angle to form a multi-pass waveguide with 5–6 total internal reflections for optical characterizations. Two types of contacts have been fabricated as

Table 1 Density, height and diameter of the quantum dots of samples S1, S2 and S3. The PL energy, intraband transition energy and photocurrent are also indicated for each sample.

	QD density ($\times 10^{11}$ cm^{-2})	height (nm)	diameter (nm)	PL energy (eV)	intraband energy and wavelength [FWHM]	photocurrent energy and wavelength
S1	6.4 ± 0.7	1.2 ± 0.6	17	3.78	0.85 eV 1.45 μm [150 meV]	0.9 eV 1.37 μm
S2	4.6 ± 0.5	1.3 ± 0.6	16	3.63	0.74 eV 1.67 μm [120 meV]	0.85 eV 1.46 μm
S3	6.8 ± 0.5	1.2 ± 0.5	15	3.9	0.84 eV 1.47 μm [150 meV]	0.88 eV 1.41 μm

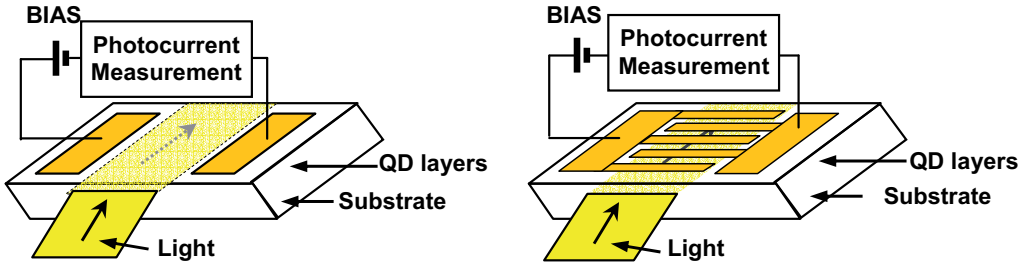

Fig. 2 (online colour at: www.pss-b.com) Scheme of the two types of photodetectors. Left: two metal contacts (900 × 3000 µm) separated by 800 µm (samples S1 and S2). Right: 20 µm wide interdigitated metal contacts separated by 10 µm or 20 µm (sample S3).

illustrated in Fig. 2. For samples S1 and S2, the two metal contacts with a size of 900 × 3000 µm are separated by 800 µm and annealed at 600 °C for 30 sec. For sample S3, interdigitated metal contacts were deposited. They consist of ten 800-µm-long and 20-µm-wide fingers, separated by 10 or 20 µm. In all cases, the metal contacts were defined by standard photolithography and the deposited metal layers are Ti/Al/Ti/Au. The linear current–voltage characteristics, shown on the inset of Fig. 3, indicate an ohmic behavior.

4 Optical measurements

Photoluminescence (PL) and Fourier transform infrared (FTIR) spectroscopy were used to investigate the optical properties of the samples S1, S2 and S3 at room temperature.

PL measurements were performed using the 244 nm line of a frequency-doubled CW Ar^{++} laser. At room temperature, the PL is peaked at 3.78 eV, 3.63 eV and 3.9 eV for S1, S2 and S3 samples, respectively. The full width at half maximum (FWHM) is less than 300 meV for the three samples which indicates a good homogeneity. Indeed, a variation of 1 monolayer of the QD height leads to a shift of ~150 meV of the PL peak energy.

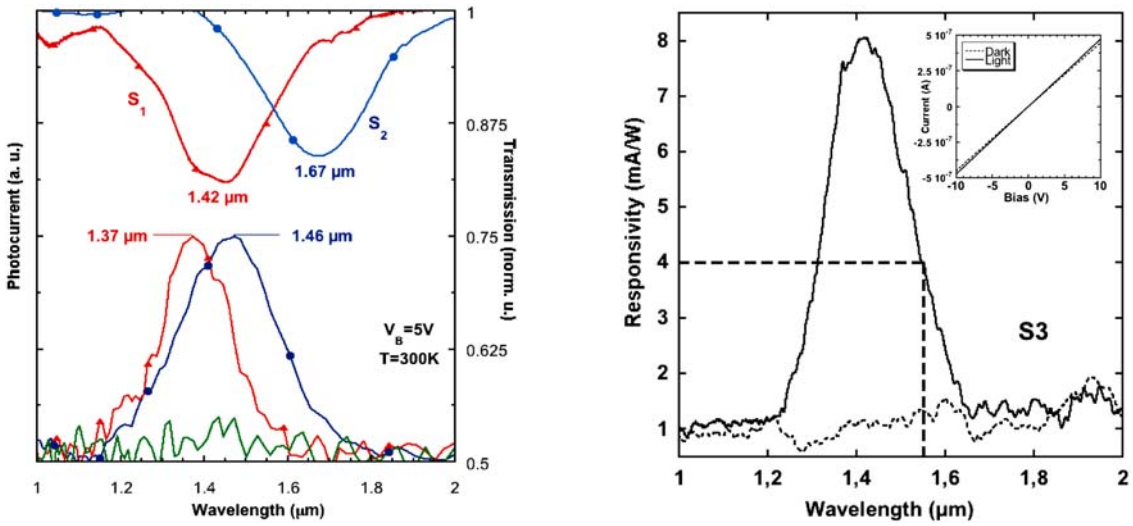

Fig. 3 (online colour at: www.pss-b.com) Left: room temperature transmission (dashed line) and photocurrent spectra (full line) for samples S1 and S2. The dotted curve shows the photocurrent for TE-polarized incident light. Right: calibrated responsivity spectrum of sample S3 peaked at 8 mA/W. Inset: current–voltage characteristics of S3 with and without illumination.

Figure 3 presents the absorption spectra of samples S1 and S2, measured with a FTIR spectrometer. The intraband absorption is peaked at 1.45 μm (0.85 eV), 1.67 μm (0.74 eV) and 1.47 μm (0.84 eV) for samples S1, S2, and S3, respectively. Absorption is only observed for TM-polarized light and not for TE-polarized light, as expected for the electronic intraband transition from the ground state (s-shell) to the excited state with one node of the envelope function along the *c*-axis (p_z-shell). The absorptions from the ground state to the in-plane excited states (p_x or p_y) are not observed in the investigated energy range, probably because their energies are below the cut-off of the sapphire substrate (0.3 eV).

5 Photocurrent measurements

The photocurrent (PC) measurements were first performed at room temperature. A continuous bias was applied to the photodetector and infrared light was injected onto the 45° angle facet at normal incidence. For samples S1 and S2, the applied bias was 5 V. The detected photocurrent was amplified with a current amplifier. We used a lock-in detection and the FTIR was operating in step-scan mode to improve the sensivity. For sample S3, the applied bias was 10 V, the intraband photocurrent was amplified and fed into the FTIR operating in rapid-scan mode. The PC responsivity has been calibrated using a 1.55 μm semiconductor laser. Figure 3 shows the PC spectra of the three samples. The PC energy peaks for each sample are indicated in Table 1. The PC responsivity for sample S3 is about 8 mA/W at 300 K.

6 Discussion

The photocurrent is only observed for TM-polarized light, following the intraband s–p_z selections rules of intraband absorption. The fact that the photocurrent obeys the same selection rules and that its spectrum closely follows the intraband absorption is clear evidence that the photocurrent originates from the intraband transition of the nitride QDs.

It should be noted that the photocurrent spectra of Fig. 3 are slightly blue shifted with respect to the s–p_z intraband absorption. The blue-shift increases with the peak wavelength of the detectors. One likely explanation supported by energy state calculations [9] is that the p_z-state is at a lower energy than the WL ground state. The difference of energy is larger for bigger dots than for smaller dots. The photoexcited electrons transfer to the wetting layer ground state via phonon absorption. The phonon-mediated mechanism favours the smaller dots in the distribution. This mechanism explains the blue-shift of the PC with respect to the absorption. It also explains why the blue-shift increases with the peak wavelength of the detection.

This interpretation is also supported by separate measurements of the photocurrent, which show an exponential increase of the PC with temperature.

7 Conclusion

We have demonstrated GaN/AlN quantum dot photodetectors based on intraband absorption and in-plane electronic transport operating at record short wavelengths for unipolar devices. The photocurrent is TM-polarized and is generated by the transfer of the photoexcited electrons from the p_z-state to the wetting layer. A blue-shift of the PC with respect to the intraband absorption is observed and is interpreted in terms of phonon-mediated transfer from the p_z-state to the ground state of the wetting layer.

References

[1] M. Tchernycheva, L. Nevou, L. Doyennette, F. H. Julien, E. Warde, F. Guillot, E. Monroy, E. Bellet-Amalric, T. Remmele, and M. Albrecht, Phys. Rev. B **73**, 125347 (2006) and references therein.

[2] Kh. Moumanis, A. Helman, F. Fossard, M. Tchernycheva, A. Lusson, F. H. Julien, B. Damilano, N. Grandjean, and J. Massies, Appl. Phys. Lett. **82**, 868 (2003).

[3] M. Tchernycheva, L. Nevou, L. Doyennette, A. Helman, R. Colombelli, F. H. Julien, F. Guillot, E. Monroy, T. Shibata, and M. Tanaka, Appl. Phys. Lett. **87**, 101912 (2005).

[4] F. Guillot, E. Bellet-Amalric, E. Monroy, M. Tchernycheva, L. Nevou, L. Doyennette, F. H. Julien, Le Si Dang, T. Remmele, M. Albrecht, T. Shibata, and M. Tanaka, J. Appl. Phys. **100**, 044326 (2006).
[5] D. Pal and E. Towe, Appl. Phys. Lett. **88**, 153109 (2006).
[6] V. Ryzhii, Semicond. Sci. Technol. **11**, 759 (1996).
[7] L. Chu, A. Zrenner, M. Bichler, and G. Abstreiter, Appl. Phys. Lett. **79**, 2249 (2001).
[8] L. Doyennette, L. Nevou, M. Tchernycheva, A. Lupu, F. Guillot, E. Monroy, R. Colombelli, and F. H. Julien, Electron. Lett. **41**, 1077 (2005).
[9] A. Vardi, N. Akopian, G. Bahir, L. Doyennette, M. Tchernycheva, L. Nevou, F. H. Julien, F. Guillot, and E. Monroy, Appl. Phys. Lett. **88**, 143101 (2006).